

# The Formation of Filamentous Carbon on Iron and Nickel Catalysts

## I. Thermodynamics

P. K. DE BOKX, A. J. H. M. KOCK, E. BOELLAARD, W. KLOP, AND J. W. GEUS

*Department of Inorganic Chemistry, State University of Utrecht, Croesestraat 77A,  
3522 AD Utrecht, The Netherlands*

Received May 31, 1984; revised July 10, 1985

The thermodynamic properties of filamentous carbon formed from CO and CH<sub>4</sub> on iron and nickel catalysts have been determined in the temperature range 650–1000 K. Catalyst samples quenched from a steady-state growth of carbon have been studied using temperature-programmed hydrogenation, thermomagnetic analysis, and electron microscopic techniques. It is concluded that carbon is deposited as a metastable carbide intermediate, leading to filamentous carbon on decomposition. The presence of carbide intermediates has been demonstrated both by magnetic measurements and by temperature-programmed hydrogenation. © 1985 Academic Press, Inc.

### INTRODUCTION

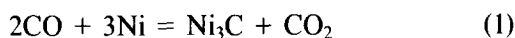
Depending on the conditions during deposition, carbon species formed on transition metal catalysts exhibit a variety of properties and morphologies (1–3). Utilizing temperature-programmed hydrogenation of carbon deposits on nickel catalysts, McCarty *et al.* (4) distinguished seven types of carbon. Using ethylene as the carbiding agent, the formation of a carbon species consisting of long filaments with metal particles at their tips was observed at temperatures between 625 and 1050 K. In this work we confine ourselves to the study of this well-documented filamentous carbon (5–7). There are two major reasons for studying this particular kind of carbon. In the first place, filamentous carbon is formed in a temperature range where reactions of great technical importance, e.g., Fischer-Tropsch synthesis, methanation, and steam-reforming, are usually carried out. Second, it is the most detrimental form of carbon. Due to its high mechanical strength filamentous carbon is capable of completely disintegrating the catalyst support structure (8), thus making all attempts at regeneration futile.

An intriguing deviation from the thermodynamic equilibrium of the carbon monoxide disproportionation reaction as predicted from data for graphite during deposition of multilayer carbon onto a nickel surface was first discovered by Dent *et al.* (9). Rostrup-Nielsen (10), studying carbon deposition reactions on nickel catalysts, identified that the carbon was filamentous. He concluded that the deviations from the graphite equilibria could be explained if both the structural disorder and the contribution of the surface energy of the high-surface-area filaments were taken into account (8, 10). Recently, Manning *et al.* (11) and Sacco and Caulmare (12), investigating the Bosch process, i.e., the reduction of CO<sub>2</sub> to carbon and water, on iron, cobalt, and nickel foils also observed deviations from graphite equilibria. An elegant phase-diagram approach was used to calculate the inlet gas compositions that are critical with respect to graphite or carbide formation. They suggested that deviations from graphite equilibria could be explained by assuming that carbon is deposited as a metastable carbide intermediate.

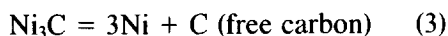
In this first study we set out to obtain quantitative data on equilibria measured

during growth of filaments as a function of temperature. To investigate the involvement of carbides in filamentous growth, two metals of known high activity (7) in carbon whisker formation were selected, i.e., iron and nickel. Two simple reactions were chosen, viz., the decomposition of methane and the disproportionation of carbon monoxide, examples of an endothermic and an exothermic reaction, respectively. The rationale for this approach will be explained for the case of nickel and carbon monoxide. The other combinations, viz., Ni/CH<sub>4</sub>-H<sub>2</sub>, Fe/CO-CO<sub>2</sub>, and Fe/CH<sub>4</sub>-H<sub>2</sub>, are analogous.

CO can react according to either of the equations



Free carbon can be formed directly due to reaction (2) or due to reaction (1) followed by



Since reaction (3) does not affect the gas-phase composition, measurement of  $K_p = p_{\text{CO}_2}/(p_{\text{CO}})^2$  yields information on the identity of the deposited solid phase (13). We have performed measurements of  $K_p$  over a range of temperatures allowing determination of both the enthalpy and the entropy of reaction. It will be shown that comparing the reaction enthalpies measured during steady-state growth of filaments with reaction enthalpies of carbide forming reactions on the one hand and reaction enthalpies of the formation of high-area graphite filaments on the other, enables us to discriminate between the above two explanations for the deviations from equilibria involving graphite.

To investigate whether carbides are present during growth of filaments, we have analyzed the solid phases. As steady-state carbide concentrations may be very low and can easily escape detection, we applied temperature-programmed hydrogenation

and thermomagnetic analysis, as well as electron microscopy.

#### EXPERIMENTAL

*Materials.* The nickel catalyst used throughout this study (50 wt% Ni/SiO<sub>2</sub>, referred to a dry, reduced sample) was dehydrated in a 10 vol% H<sub>2</sub>/N<sub>2</sub> flow at 393 K and consecutively reduced for at least 72 h at 723 K. To avoid a continuation of the reduction during subsequent experiments, reduced catalyst samples were exposed to 10 vol% H<sub>2</sub>/N<sub>2</sub> during 1 h at 950 K. Average particle sizes of the nickel catalyst were obtained using magnetic methods after hydrogenation of deposited carbon. The mean dispersion is estimated to be 0.1, the Langevin low-field estimate for the mean particle size being 5.4 nm (15), assuming the particles are spherical.

The iron catalyst (50 wt% Fe/Al<sub>2</sub>O<sub>3</sub>) was prepared by depositing Fe(OH)<sub>3</sub> onto a  $\gamma$ -alumina support (Degussa C). Precipitation was achieved by means of slow injection of an iron(III) nitrate solution into a suspension of the support. The pH of the suspension was kept at a value of 6.0. The catalyst was reduced in a 10 vol% H<sub>2</sub>/Ar mixture at 873 K for at least 10 h. Again the catalyst was exposed to higher temperatures to avoid a continuation of the reduction during equilibration experiments. The average particle size of the iron catalyst could not be obtained by magnetic granulometry as the catalyst sample did not show superparamagnetic behavior. The average particle size of the iron catalyst was determined after hydrogenation of deposited carbon and was estimated to be 25 nm using the Scherrer equation for X-ray line broadening [Fe(110) reflection].

All gases, except methane, were obtained from Hoek-Loos Company and were passed successively through columns containing a Deoxo catalyst (BASF R-3-11) and a molecular sieve (Linde 4A) to remove traces of oxygen and water, respectively. Methane was supplied by Matheson Company as a calibrated methane/nitrogen mix-

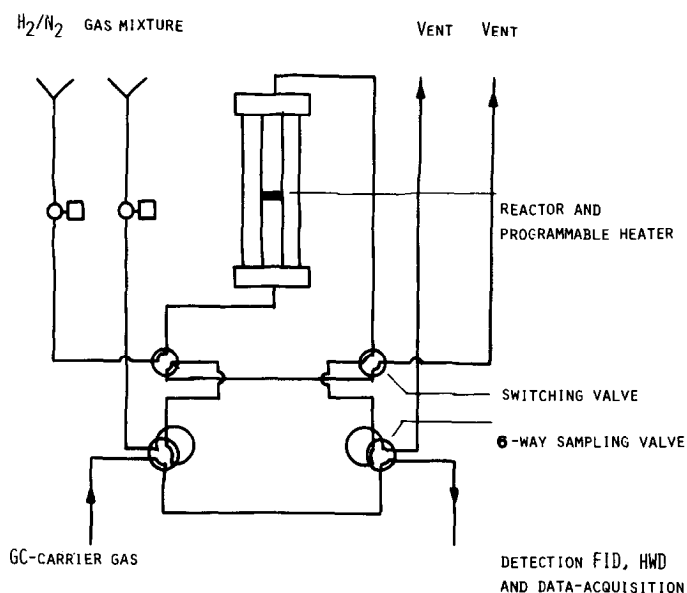


FIG. 1. Schematic diagram of the flow apparatus.

ture. It was used without further purification. Methanol (Baker p.a.) could be introduced into the feed at accurately known concentrations using a device described by Davydov and Kharson (16).

**Apparatus and procedure.** To study equilibria during carbon deposition a continuous-flow system was employed (Fig. 1). Gas mixtures, typically containing between 1 and 10 vol% carbon-bearing gas, were prepared in a gas mixing system. The mixture was fed to a quartz reactor (i.d. 10 mm) containing between 1 and 3 g of the pelleted catalyst (0.15–0.30 mm). Samples were drawn from the gas flow using pneumatic sampling valves (Valco). Gas chromatographic analysis of the samples was performed using a Perkin–Elmer Sigma 1 chromatograph. Separation was normally carried out over a 3.0-m stainless-steel column packed with Porapak QS isothermally operated at 333 K. When methanol was used as a reactant, a temperature program was employed up to 413 K. Quantitative analyses were obtained using a hot-wire detector (HWD) and a flame ionization detector (FID) in series. Between the HWD and the FID a catalytic reactor (Perkin–

Elmer) was installed to convert CO and CO<sub>2</sub> quantitatively to CH<sub>4</sub>, thereby greatly increasing detection sensitivity ( $\pm 0.1$  ppm). The reactant flow could be instantaneously replaced by an inert gas flow by means of two four-way valves. This procedure was applied during quenching from steady-state growth.

Catalyst samples were reduced *in situ* and flushed with N<sub>2</sub> for 2 h at 873 K to remove adsorbed H<sub>2</sub>. A carburizing gas mixture was fed to the catalyst until steady-state carburizing was observed. Subsequently, the flow rate was lowered stepwise until effluent compositions ceased to be a function of the residence time. The gas composition thus obtained was taken to be the equilibrium composition. Samples were subjected to a forced cool-down in N<sub>2</sub> to room temperature, typically within 120 s, and were then analyzed with regard to the solid phases present.

**Analysis of the solid phases.** Temperature-programmed hydrogenation (TPH) of the carbon deposits was performed using a 10 vol% H<sub>2</sub>/N<sub>2</sub> mixture at a total flow rate of 1 cm<sup>3</sup> s<sup>-1</sup>. The only product observed was methane. Its evolution was discontinu-

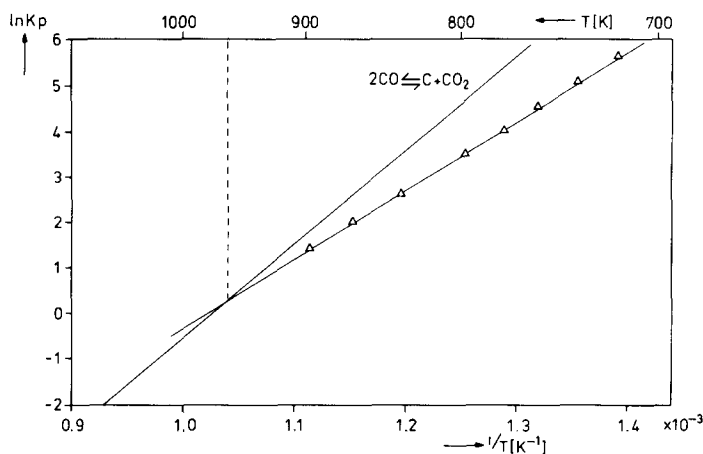


FIG. 2. Measured equilibrium constants for CO disproportionation on a 50 wt% Ni/SiO<sub>2</sub> catalyst (triangles). Equilibria based on graphite data are also indicated.

ously recorded as a function of temperature using GC analysis. Due to the time required for one analysis (0.42 ks), linear heating rates were limited to 11 mK s<sup>-1</sup>.

Thermomagnetic analysis (TMA) of carbided samples could be performed using a modified Weiss-extraction technique (magnetic fields up to 0.52 MA m<sup>-1</sup>) in the temperature range 100–740 K (17). Saturation magnetizations could be measured in the same quartz reactor used in equilibrium and TPH experiments. Ferromagnetic carbides present in the samples could be identified on the basis of Curie temperatures.

Filamentous carbon could be directly observed in Philips EM 420 and Jeol 200C electron microscopes. Samples were passivated in air statically, ultrasonically treated in ethanol, and dispersed over a holey carbon film. Both microscopes were equipped with facilities for selected area electron diffraction (SAED). In some cases X-ray diffraction (XRD) patterns were obtained using a Philips PW 1140 diffractometer.

## RESULTS

### Nickel Catalysts

In Figs. 2 and 3 the logarithms of the measured equilibrium constants have been plotted as a function of the reciprocal tem-

perature. Straight lines through the data points have been obtained using an unweighted least-squares fit. For both reactions deviations from the equilibria based on graphite data are observed. It is interesting to note that the measured lines in Figs. 2 and 3 intersect at high temperatures with lines representing graphite equilibria.

In Fig. 4 a typical TPH profile of a catalyst sample quenched from steady-state

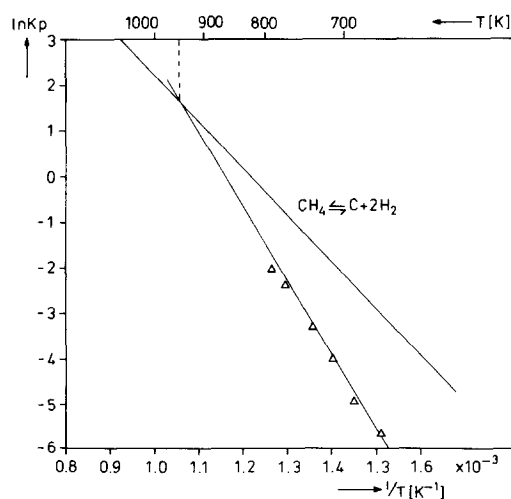


FIG. 3. Measured equilibrium constants for CH<sub>4</sub> decomposition on a 50 wt% Ni/SiO<sub>2</sub> catalyst (triangles). Equilibria for CH<sub>4</sub> decomposition based on graphite data are also indicated.

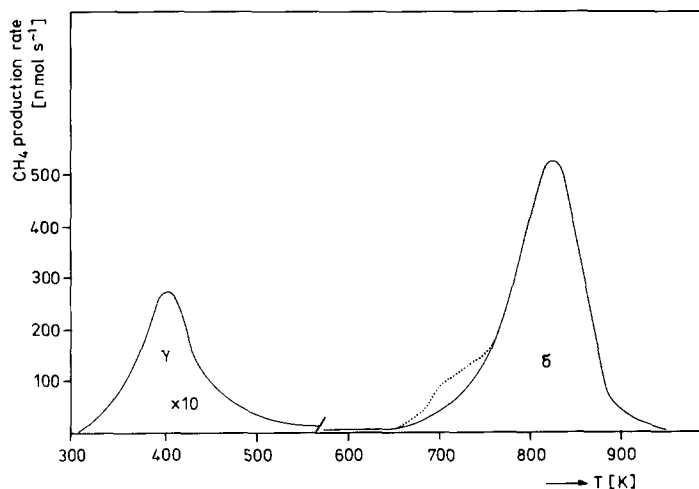


FIG. 4. Temperature-programmed hydrogenation profile of a 50 wt% Ni/SiO<sub>2</sub> catalyst, after steady-state carburization by exposure to CH<sub>4</sub> at 750 K (heating rate: 11 mK s<sup>-1</sup>, flow rate: 1.0 cm<sup>3</sup> s<sup>-1</sup> 10 vol% H<sub>2</sub>/N<sub>2</sub>).

growth is shown. The high-temperature peak (825 K) increased with increasing carburization time and could be made to attain values corresponding to carbon/nickel mole ratios of more than 10. It was identified with filamentous carbon by means of electron microscopy (Fig. 5). Although the position of the peak maximum of the low-temperature peak and the total carbon content (1.5–6 at.%) would suggest an adsorbed carbon species (4), at least part of the carbon corresponding to the low-temperature peak is located in the bulk of the metal. This can be appreciated from two arguments based on magnetic measurements. First, the saturation magnetization decreased up to 30% after carburization, which is about three times the decrease expected for adsorption of a complete monolayer, i.e., a decrease corresponding to the dispersion (0.1). The second argument can be derived from Fig. 6. It is seen that the thermomagnetic curve measured on heating the sample does not coincide with the curve measured on cooling. The former curve, moreover, does not exhibit the expected temperature dependence of the magnetization at temperatures around 430 K. The explanation for this phenomenon, following

Escoubes and Eyraud (18), is the decomposition of the paramagnetic nickel carbide Ni<sub>3</sub>C. It should be emphasized that TMA was performed on a sample quenched from a steady-state growth of carbon. Thus, although some carbon may actually be present as a surface carbide, we must conclude that a substantial fraction is present in the bulk of the nickel particle. Using selected-area electron diffraction of carburized samples no other compounds than graphite and metallic nickel could be detected.

It should be noted that steady-state growth was not observed in all cases. High partial pressures of CO combined with high temperatures led to a fast deactivation of both nickel and iron catalysts. TPH of these deactivated catalysts showed a shoulder (dashed in Fig. 4) on the low-temperature side of the peak due to filamentous carbon. Due to the low heating rate used in this work (11 mK s<sup>-1</sup>), the peak temperatures are significantly lower than the temperatures of similarly labeled peaks reported by McCarty *et al.*, who utilized a heating rate of about 1 K s<sup>-1</sup> (3, 4). Considering the relative stabilities of the various carbon species, this shoulder may be attributed to

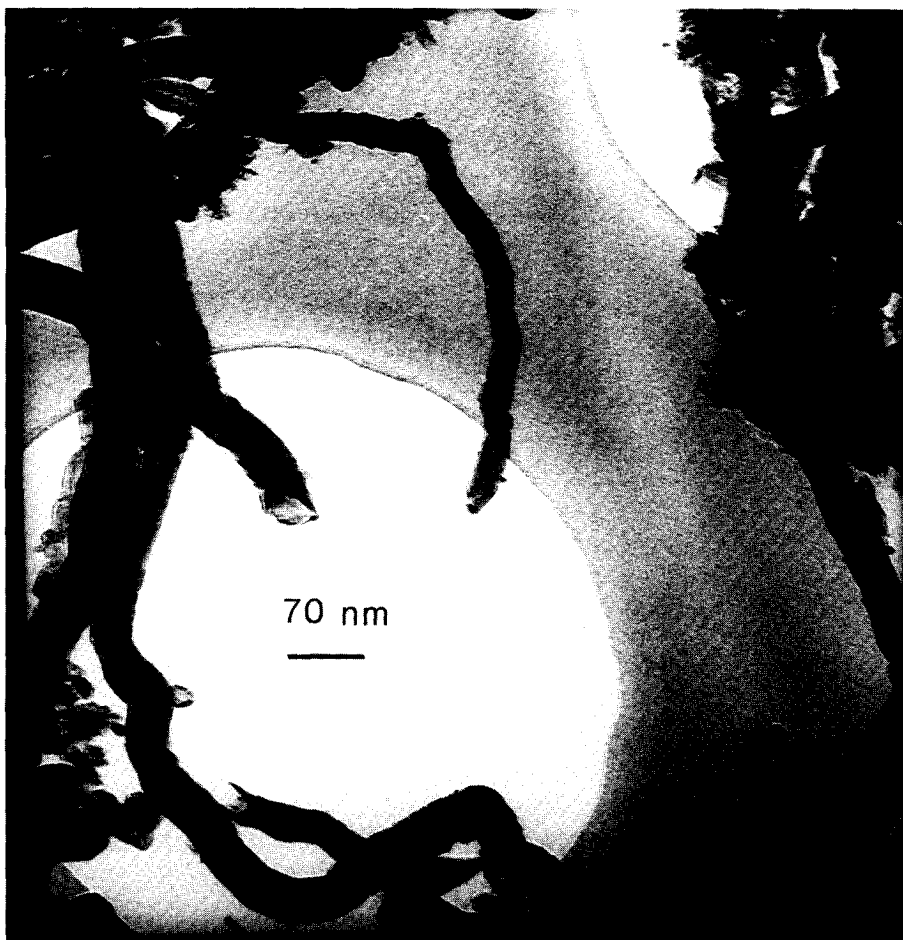


FIG. 5. Electron micrograph of a 50 wt% Ni/SiO<sub>2</sub> catalyst, after steady-state carburization by exposure to CH<sub>4</sub> at 750 K.

amorphous carbon ( $\beta$ -carbon according to Ref. (4)).

#### *Iron Catalysts*

Figures 7 and 8 illustrate the deviations from equilibria based on graphite data observed on iron catalysts. Extensive filament formation occurred during these measurements (Fig. 9). Temperature-programmed hydrogenation and selected-area electron diffraction, as well as X-ray diffraction, only revealed the presence of cementite ( $\theta$ -Fe<sub>3</sub>C), metallic iron, and graphite in the samples. As can be seen from Fig. 10 thermomagnetic analysis also demonstrates cementite formation under growth conditions.

In a few experiments methanol was used as the carburizing agent. It was found that iron shows a higher affinity to formation of carbon filaments than does nickel. There are sets of conditions, e.g.,  $p_{\text{CH}_3\text{OH}} = 7$  kPa and  $T = 773$  K, where filamentous growth proceeds on iron, whereas on nickel no filament formation is observed.

#### DISCUSSION

##### *Nickel Catalysts*

The equilibrium data of Figs. 2 and 3 have been interpreted using a zeroth order approximation, i.e., the temperature dependences of enthalpy and entropy have been neglected. This approach leads to de-

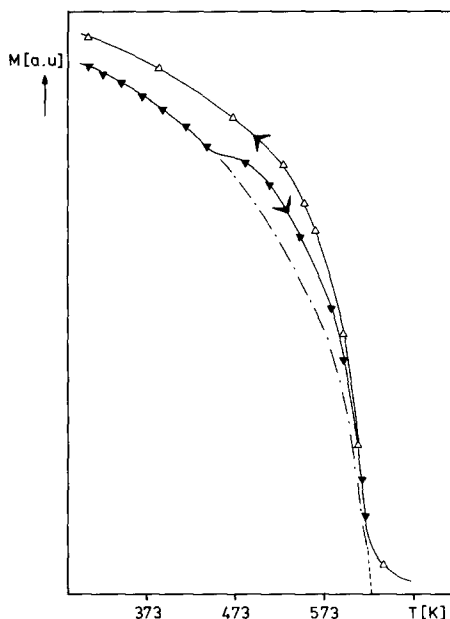


FIG. 6. Thermomagnetic analysis of a 50 wt% Ni/SiO<sub>2</sub> catalyst in a He atmosphere at increasing (solid triangles) and decreasing (open triangles) temperature, after steady-state carburization by exposure to CH<sub>4</sub> at 820 K (heating rate 0.1 K s<sup>-1</sup>).

viations from more accurate approximations of thermodynamic functions. In the temperature range of our experiments, however, these deviations are well within the error bounds of the reported values for the compounds under consideration (20).

Reaction enthalpies and entropies for the nickel catalyzed reactions are collected together with literature data on nickel carbide in Table 1. Deviations from graphite data are again apparent. It is seen that the calculated values for the reaction enthalpy during filament growth correspond well with the enthalpy change for the reactions



The reaction entropies show a larger spread. The reported literature values are, however, far from accurate. Errors in Gibbs free energy values are seldom reported and the way in which the accuracy of the reaction enthalpies and entropies is affected cannot be deduced easily. However, it should be mentioned that the values we obtained for the Gibbs free energy (not to be confused with the Gibbs free energy of formation) of Ni<sub>3</sub>C from the two independent reactions are internally consistent (Table 2). A plausible physical explanation for the difference between the reported entropy of nickel carbide (21) and our experimentally observed value is the substoichiometric nature of the formed nickel carbide (carbon contents: 1.5–6 at.%).

In view of the essentially different expla-

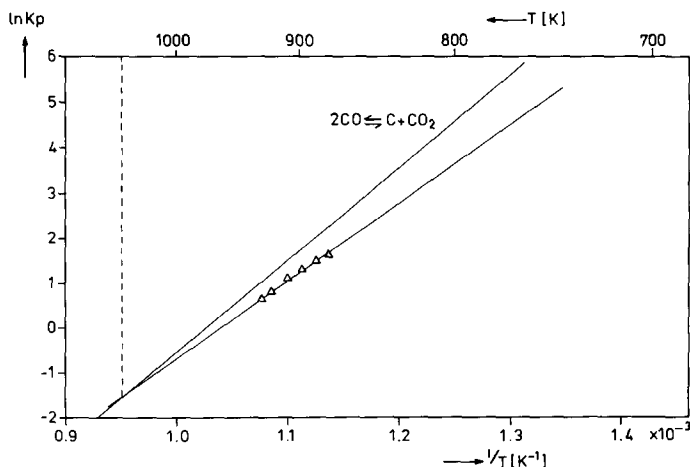


FIG. 7. Measured equilibrium constants for CO disproportionation on a 50 wt% Fe/Al<sub>2</sub>O<sub>3</sub> catalyst (triangles). Equilibria for CO disproportionation based on graphite data are also indicated.

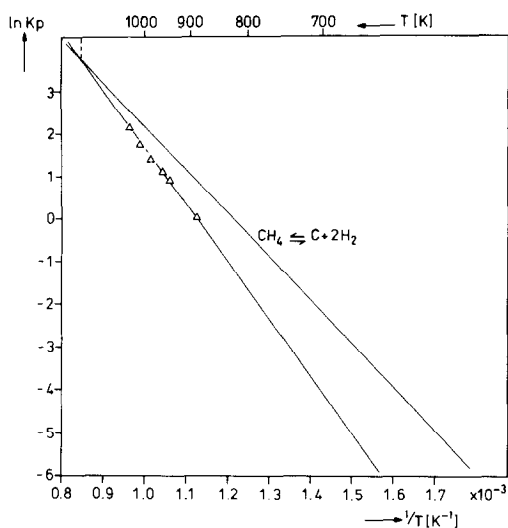


FIG. 8. Measured equilibrium constants for  $\text{CH}_4$  decomposition on a 50 wt% Fe/Al<sub>2</sub>O<sub>3</sub> catalyst (triangles). Equilibria for  $\text{CH}_4$  decomposition based on graphite data are also indicated.

nation offered by Rostrup-Nielsen (10) for deviations from graphite equilibria, the good correlation of his data with those reported for Reaction (4) is striking (Table 1). In our opinion, his explanation, i.e., deviations from graphite equilibria due to contributions of surface energy and structural disorder, can be ruled out. This can be understood by focusing on the difference between the experimental reaction enthalpy and that corresponding to the graphite equilibrium. In the Appendix it is demonstrated that the contribution of the surface energy does not lead to differences in reaction enthalpy larger than  $7.5 \text{ kJ mol}^{-1}$ . It should be emphasized that the filament diameter (10 nm) used in the calculation of the surface energy contribution corresponds to the minimum diameter observed in electron micrographs. The value used for the surface enthalpy corresponds to graphite surfaces

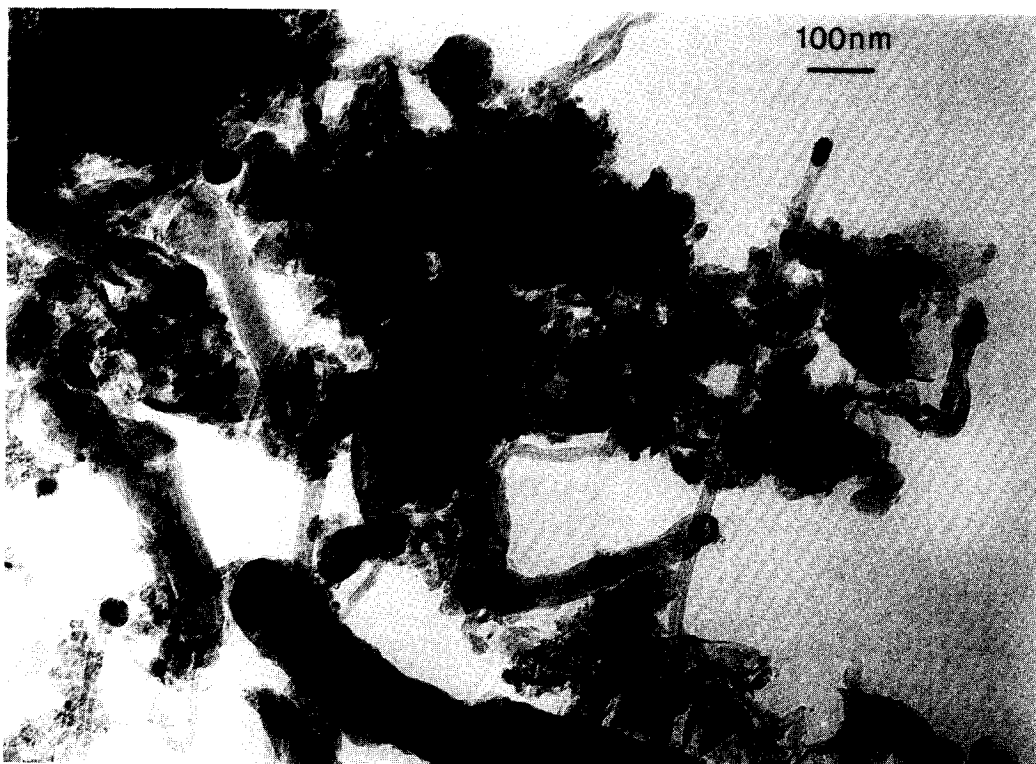


FIG. 9. Electron micrograph of a 50 wt% Fe/Al<sub>2</sub>O<sub>3</sub> catalyst, after steady-state carburization by exposure to CO at 900 K.

TABLE 1

Comparison of the Thermodynamic Functions for CO Disproportionation and CH<sub>4</sub> Decomposition on Nickel

Reaction	$\Delta H_r$ (kJ mol <sup>-1</sup> )	$\Delta S_r$ (J mol <sup>-1</sup> K <sup>-1</sup> )	Ref.
CH <sub>4</sub> (g) = C(s) + 2H <sub>2</sub> (g)	84.5	105	21
3Ni(s) + CH <sub>4</sub> (g) = Ni <sub>3</sub> C(s) + 2H <sub>2</sub> (g)	124.6	121.3	18, 22
	131 ± 4	149 ± 6	This work
2CO(g) = C(s) + CO <sub>2</sub> (g)	-172.4	-177.4	21
3Ni(s) + 2CO(g) = Ni <sub>3</sub> C(s) + CO <sub>2</sub> (g)	-133.1	-160.6	18, 22
	-133.9	-146.4	10
	-126 ± 1	-129 ± 2	This work

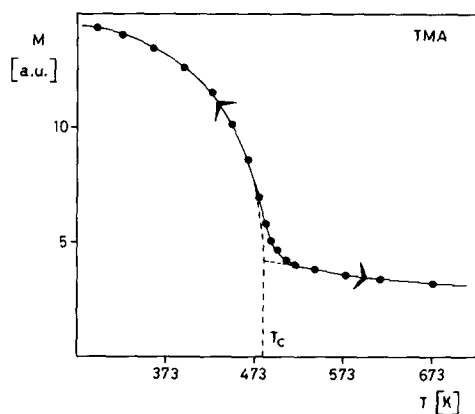


FIG. 10. Thermomagnetic analysis of a 50 wt% Fe/Al<sub>2</sub>O<sub>3</sub> catalyst in a He atmosphere at increasing and decreasing temperature, after steady-state carburization by exposure to CO at 900 K. Heating rate: 0.1 K s<sup>-1</sup>. The Curie temperature ( $T_c$ ) of cementite ( $482 \pm 7$  K) (19) is indicated.

perpendicular to the graphite basal plane. Surface enthalpies for graphite range from 0.16 J m<sup>-2</sup> for the graphite basal plane to 6.3 J m<sup>-2</sup> for planes perpendicular to the (0001) planes (34, 35). As we have used both the smallest filament diameter and the highest reported surface enthalpy in our calculation, the value of 7.5 kJ mol<sup>-1</sup> should be regarded as an upper limit estimate of the contribution of the surface enthalpy. The experimentally observed difference, however, is approximately 40 kJ mol<sup>-1</sup>. Rosstrup-Nielsen introduced a parameter  $\mu^*$  to account for the structural disorder of the carbon filaments compared to graphite. The temperature dependence of the difference between the experimentally observed equilibrium constants and those calculated from

TABLE 2

Gibbs Free Energy Values of Nickel Carbide

T (K)	$G_{\text{Ni}_3\text{C}}$ (kJ mol <sup>-1</sup> )	
	Calculated from methane decomposition data	Calculated from carbon monoxide disproportionation data
600	-49 ± 5	-51.0 ± 1.7
700	-72 ± 6	-73.2 ± 1.7
800	-96 ± 6	-97.5 ± 1.7
900	-120 ± 7	-122.6 ± 2.1

bulk graphite data was attributed to an increase of the structural order with increasing temperature, i.e., to the temperature dependence of  $\mu^*$ . In other words, the enthalpy difference between carbon phases of different structural order was invoked to explain the observation that deviations from graphite equilibria decrease with increasing temperature (Figs. 2 and 3). However, the heats of oxidation of natural graphite and amorphous carbon, illustrating two extremes of carbon order, do not differ by more than  $15 \text{ kJ mol}^{-1}$  (24). Hence, the contributions of both the degree of carbon order and the surface energy of the filaments cannot account for differences in the reaction enthalpy exceeding  $22.5 \text{ kJ mol}^{-1}$ .

It appears that the explanation proposed by Manning *et al.* (11) is correct. Carbon is deposited as an intermediate carbide, which can decompose either into carbon and a carbide of lower carbon content or into carbon and fcc nickel. The complete decomposition into carbon and fcc nickel (which is thermodynamically most attractive) does not proceed easily. As a result, the reverse reaction, i.e., decarburization, can be expected to proceed via the same metastable carbide intermediate as long as complete decomposition into carbon and fcc nickel has not been effected. Accordingly, the same equilibrium has been measured both under carburizing and decarburizing conditions (10). However, the same (carbide) equilibrium is obtained only if conditions are gradually changed from carburization to decarburization. If, on the other hand, the carbide is allowed to decompose completely before exposing the sample to decarburizing conditions, equilibria involving graphite are measured during decarburization, whereas carbide equilibria are attained during carburization (13). Thus, as long as a metastable carbide is present, the kinetically attractive route via an intermediate carbide phase remains accessible. Moreover, the formation of a carbide from graphite and carbide of low carbon content is expected to be more

favorable than that from graphite and nickel. The observations of Bromley and Strickland-Constable (13) indicate that the formation of nickel carbide from fcc nickel and graphite does not proceed.

It should be noticed that the differences in stability between nickel carbide and its constituent elements become negligibly small at elevated temperatures (the points of intersection in Figs. 2 and 3). Any mechanism involving carbide decomposition is thus thermodynamically limited to a maximum temperature.

### *Iron Catalysts*

In Table 3 the data obtained in the presence of iron catalysts are collected. The interpretation is greatly hampered by the existence of a number of iron carbides. To the best of our knowledge, thermodynamic functions of only two iron carbides are known, namely cementite ( $\theta\text{-Fe}_3\text{C}$ ) and a carbide reported to be  $\text{Fe}_2\text{C}$  by Browning *et al.* (25). The latter carbide was shown to be  $\chi\text{-Fe}_5\text{C}_2$  by X-ray diffraction (26). Our results seem to coincide nicely with the data reported for cementite. Due to the limited accuracy of the literature data on carbides care should be taken in discriminating between possible intermediates on the basis of the values of their thermodynamic functions. The question as to which iron carbide is the intermediate in, or catalyst for, filamentous growth is a matter of some controversy (27) and will be dealt with in Part II (17). Iron carbides could also have formed from CO reduction of oxides, e.g.,  $\text{FeO}$ ,  $\text{Fe}_3\text{O}_4$  (28). Interference of these equilibria can be ruled out on the basis of the observed partial pressures of CO and  $\text{CO}_2$ . The observation that carbide data derived from methane decomposition on the one hand, and from carbon monoxide disproportionation on the other, were identical within experimental error, also shows that the involvement of simultaneous reduction and carburization reactions is not significant. Although identification of the iron carbide intermediate is not possible on the

TABLE 3  
Comparison of Thermodynamic Functions for CO Disproportionation and CH<sub>4</sub> Decomposition on Iron

Reaction	$\Delta H_r$ (kJ mol <sup>-1</sup> )	$\Delta S_r$ (J mol <sup>-1</sup> K <sup>-1</sup> )	Ref.
CH <sub>4</sub> (g) = C(s) + 2H <sub>2</sub> (g)	84.5	105	21
2Fe(s) + CH <sub>4</sub> (g) = Fe <sub>2</sub> C(s) + 2H <sub>2</sub> (g)	105.4	113.8	18, 19
3Fe(s) + CH <sub>4</sub> (g) = Fe <sub>3</sub> C(s) + 2H <sub>2</sub> (g)	111.7	128.9	18, 19, 22
	114 ± 6	130 ± 7	This work
2CO(g) = C(s) + CO <sub>2</sub> (g)	-172.4	-177.4	21
2Fe(s) + 2CO(g) = Fe <sub>2</sub> C(s) + CO <sub>2</sub> (g)	-152.7	-167.4	18, 19
3Fe(s) + 2CO(g) = Fe <sub>3</sub> C(s) + CO <sub>2</sub> (g)	-145.6	-150.6	18, 19, 22
	-138 ± 8	-143 ± 9	This work

basis of the present results, it is evident that a mechanism in which carbon is deposited as a carbide intermediate is entirely consistent with the data obtained. The observed presence of carbon contents far higher than the reported solubilities of carbon in iron supports this contention.

The observed difference in affinity for deposition of carbon between iron and nickel catalysts can also be explained by assuming that carbide intermediates are required for filamentous growth. This is illustrated in Fig. 11. Here the phase-diagram approach introduced by Manning and Reid (28) is employed. The solid lines in the ternary diagrams represent equilibria with graphite. They divide the triangle of possible compositions into two regions, namely

compositions thermodynamically favoring graphite formation (above the line), and a region where graphite formation is thermodynamically impossible (below the line). The dashed lines analogously divide the composition triangle into regions where carbide formation is favored, and where it is not possible, respectively. The carbide lines have been calculated using the data obtained from our equilibration experiments. It can be seen from Fig. 11 that under the specified conditions the point referring to methanol lies above the carbide line with iron catalysts and below the line with nickel catalysts. No filamentous growth was observed under conditions where carbide formation is thermodynamically impossible.

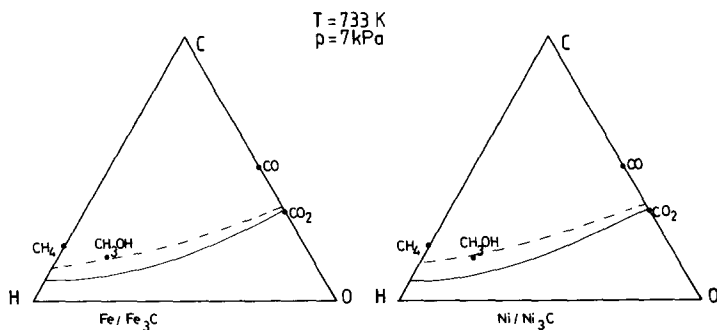


FIG. 11. C-H-O phase diagrams, containing graphite-gas (solid lines) and carbide-gas equilibria (dashed lines). Note the position of the points referring to methanol relative to the carbide lines.

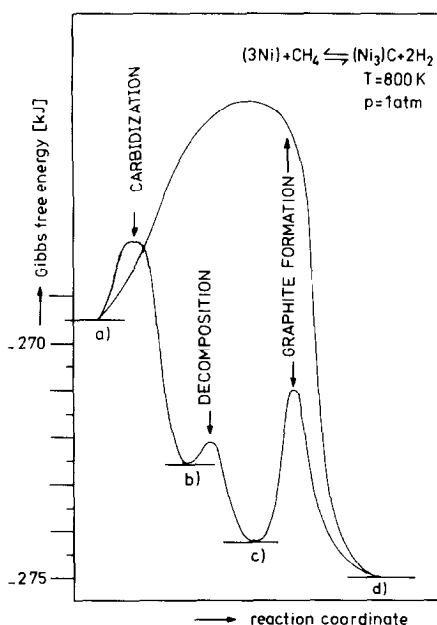


FIG. 12. Representation of the Gibbs free energy content of a system composed of (a) 1 mol Ni and 1 mol  $\text{CH}_4$ ; (b) after attainment of the  $\text{Ni}/\text{Ni}_3\text{C}/\text{CH}_4/\text{H}_2$  equilibrium; (c) after decomposition of the formed  $\text{Ni}_3\text{C}$ ; (d) after attainment of the  $\text{Ni}/\text{C}(\text{graphite})/\text{CH}_4/\text{H}_2$  equilibrium.

This conclusion has some important consequences for filament-free operation. It implies that higher contents of carbon-bearing gases are allowed than corresponding to graphite equilibria, assuming all gas-phase reactions to be at equilibrium, the so-called principle of the equilibrated gas (8). The applicability of this principle has been questioned (30). It has been stated that rates of carbon deposition are higher than rates of carbon removal, mainly based on the observation that rates of oxidation and hydrogenation of graphite are quite low in the temperature range under consideration. Given the new insight that not the rates of hydrogenation and oxidation of graphite, but the rates of hydrogenation and oxidation of a metal carbide determine the attainment of equilibrium, a reevaluation of the applicability of the principle seems necessary. It should be emphasized that experiments in which deviations were reported have been

conducted in adiabatic reactors, whereas the principle was confirmed in experiments where temperature was accurately controlled. A second consequence of the carbide intermediate model is that filament growth can be suppressed if catalysts are used that have low affinity for carbide formation, e.g., ruthenium (31). In the opinion of the present authors, alloys, e.g., Cu–Ni and Cu–Fe, provide promising alternatives to monometallic catalysts.

Finally, we would like to comment on a long discussion in the literature as to which solid phase catalyses filamentous growth. Our findings are summarized in Fig. 12. The level designated (a) corresponds to 1 mol of nickel and 1 mol of methane. Level (b) is the Gibbs free energy of the system when an equilibrium amount of nickel carbide has formed and level (c) the Gibbs free energy when the nickel carbide formed at (b) decomposes to carbon and nickel. On going from (b) to (c) the gas-phase composition obviously remains unchanged. Level (d), the equilibrium with graphite, is not reached under our conditions due to the high activation barrier for the homogeneous nucleation of graphite (32). As the positions of levels (b) and (c) are determined by the thermodynamic constants of the metal carbides considered, the process of filamentous growth is not catalytic according to the classic Ostwald definition (33). It is a heterogeneous reaction in which the product, a metastable carbide, decomposes into its constituent elements. The identification of the metastable carbides as well as the mechanism by which the carbides decompose remain subjects of great interest and will be dealt with in Part II.

## CONCLUSIONS

(i) The carbon leading to filamentous carbon is deposited as a metastable carbide intermediate.

(ii) The process in which filamentous carbon is formed should not be referred to as catalytic. It concerns a heterogeneous reaction with a decomposing product.

## APPENDIX

In this section we aim to calculate the difference in reaction enthalpy between graphite-forming and carbon-filament-forming reactions, resulting from the contribution of the surface energy of the filaments. The chemical potential of a substance  $j$  present in a solid phase  $\alpha$  at constant temperature is given by

$$\mu_j^\alpha(p_\alpha) = \mu_j^\alpha(p = 1) + v_j(p_\alpha - 1), \quad (\text{A-1})$$

where  $v_j$  is the molar volume of the substance  $j$ . If the phase is in mechanical equilibrium with the gas-phase  $\beta$ , separated by a curved interface, the pressures  $p_\alpha$  and  $p_\beta$  are related by the Laplace equation

$$p_\alpha = p_\beta + \gamma(T) \cdot (1/r_1 + 1/r_2), \quad (\text{A-2})$$

where  $\gamma(T)$  is the surface tension of the solid-gas interface and  $r_1$  and  $r_2$  are the radii of curvature.

In the case of a cylindrical interface and a total gas pressure  $p = 1$  atm, Eqs. (A-1) and (A-2) combine to

$$\mu_j^\alpha = \mu_j^\alpha(p = 1) + v_j\gamma(T)/r. \quad (\text{A-3})$$

For a given carbon-forming reaction the difference in Gibbs free energy change between the formation of carbon filaments of radius  $r$  and platelet graphite is thus equal to  $v_C\gamma(T)/r$ , assuming that the filaments formed are also graphitic. Thus, we have:

$$RT \ln K_p^*/K_p = -v_C\gamma(T)/r, \quad (\text{A-4})$$

where  $K_p^*$  is the equilibrium constant for the formation of filamentous carbon and  $K_p$  is the equilibrium constant associated with the formation of platelet graphite.

Dividing (A-4) by  $RT$  and differentiating with respect to  $1/T$  one obtains

$$\Delta H^* - \Delta H = v_C\gamma(T)/r - v_C T/r \cdot d\gamma(T)/dT. \quad (\text{A-5})$$

Writing  $\gamma$  as  $\gamma(T) = \varepsilon - T\sigma$ , where  $\varepsilon$  is the surface enthalpy and  $\sigma$  is the surface entropy, and substituting for  $\gamma(T)$  in expression (A-5), we have

$$\Delta H^* - \Delta H = v_C\varepsilon/r. \quad (\text{A-6})$$

The temperature dependence of enthalpy and entropy terms was neglected in the derivation of (A-6). Assuming cylindrical filaments ( $6.0 \text{ cm}^3/\text{mol}$ ) of diameter 10 nm and a surface enthalpy ( $\varepsilon$ ) of  $6.3 \text{ J m}^{-2}$  (34) we obtain a value of  $\Delta H^* - \Delta H$  of only  $7.5 \text{ kJ mol}^{-1}$ .

## ACKNOWLEDGMENTS

The authors are indebted to Mr. G. H. Verhoeckx and Dr. O. L. J. Gijzeman for helpful discussions. The investigations were financially supported by the VEG Gasinstituut n.v. and by the Netherlands Organization for the Advancement of Pure Research (ZWO).

## REFERENCES

1. Bartholomew, C. H., *Catal. Rev.-Sci. Eng.* **24**, 67 (1982).
2. Trimm, D. L., *Catal. Rev.-Sci. Eng.* **16**, 155 (1977).
3. McCarty, J. G., and Wise, H., *J. Catal.* **57**, 406 (1979).
4. McCarty, J. G., Hou, P. Y., Sheridan, D., and Wise, H., in "Coke Formation on Metal Surfaces" (L. F. Albright and R. T. K. Baker, Eds.), ACS Symposium Series 202, p. 253. Amer. Chem. Soc., Washington, D.C., 1982.
5. Baker, R. T. K., *Catal. Rev.-Sci. Eng.* **19**, 161 (1979).
6. Rostrup-Nielsen, J. R., and Trimm, D. L., *J. Catal.* **48**, 155 (1977).
7. Baker, R. T. K., Yates, D. J. C., and Dumesic, J. A., in "Coke Formation on Metal Surfaces" (L. F. Albright and R. T. K. Baker, Eds.), ACS Symposium Series 202, p. 1. Amer. Chem. Soc., Washington, D.C., 1982.
8. Rostrup-Nielsen, J. R., in "Catalysis, Science and Technology" (J. R. Anderson and M. Boudart, Eds.), Vol. 5, p. 3. Springer, Berlin, 1984.
9. Dent, F. J., Moignard, L. A., Eastwood, A. H., and Blackburn, W. H., *Trans. Inst. Gas Eng.*, 602 (1945-46).
10. Rostrup-Nielsen, J. R., *J. Catal.* **27**, 343 (1972).
11. Manning, M. P., Garmirian, J. E., and Reid, R. C., *Ind. Eng. Chem. Process Des. Dev.* **21**, 404 (1982).
12. Sacco, A., Jr., and Caulmare, J. C., in "Coke Formation on Metal Surfaces" (L. F. Albright and R. T. K. Baker, Eds.), ACS Symposium Series 202, p. 177. Amer. Chem. Soc., Washington, D.C., 1982.
13. Bromley, J., and Strickland-Constable, R. F., *Trans. Faraday Soc.* **56**, 1492 (1960).
14. Hermans, L. A. M., and Geus, J. W., in "Studies of Surface Science and Catalysis" (P. Delmon, P. Grange, P. Jacobs, and G. Poncelet, Eds.), p. 113. Elsevier, Amsterdam, 1979.

15. Selwood, P. W., "Chemisorption and Magnetization." Academic Press, New York, 1975.
16. Davydov, E. M., and Kharson, M. S., *Zh. Fiz. Khim.* **50**, 2984 (1976).
17. Kock, A. J. H. M., de Bokx, P. K., Boellaard, E. Klop, W., and Geus, J. W., *J. Catal.* **96**, 468 (1985).
18. Escoubes, M., and Eyraud, C., *Bull. Soc. Chim. Fr.*, 1374 (1966).
19. Loktev, S. M., Makarenkova, L. I., Slivinskii, E. V., and Entin, S. D., *Kinet. Katal.* **13**, 1042 (1971).
20. Richardson, F. D., *J. Iron Steel Inst.* **175**, 33 (1953).
21. Browning, L. C., and Emmett, P. H., *J. Amer. Chem. Soc.* **74**, 1680 (1952).
22. Barin, I., and Knacke, O., "Thermochemical Properties of Inorganic Substances." Springer, Berlin, 1973.
23. Barin, I., Knacke, O., and Kubaschewski, O., "Thermodynamical Properties of Inorganic Substances: Supplement." Springer, Berlin, 1977.
24. Mantell, L. C., "Carbon and Graphite Handbook." Interscience, New York, 1968.
25. Browning, L. C., DeWitt, T. W., and Emmett, P. H., *J. Amer. Chem. Soc.* **72**, 4211 (1950).
26. Senateur, J. P., Fruchart, R., and Michel, A., *C. R. Acad. Sci. Paris* **255**, 1615 (1962).
27. Sacco, A., Jr., Thacker, P., Chang, T. N., and Chiang, A. T. S., *J. Catal.* **85**, 224 (1984).
28. Manning, M. P., and Reid, R. C., *Ind. Eng. Chem. Process Des. Dev.* **16**, 358 (1977).
29. Audier, M., Coulon, M., and Bonnetain, L., *Carbon* **21**, 93 (1983).
30. White, G. A., Rozkowski, T. R., and Stanbridge, D. W., *Hydrocarbon Process.*, 130 (1975).
31. Toth, L. E., in "Refractory Materials" (J. L. Margrave, Ed.), Vol. 1, p. 2. Academic Press, New York, 1971.
32. Lobo, L. S., Trimm, D. L., and Figueiredo, J. C., in "Proceedings, 5th International Congress on Catalysis, Palm Beach, 1972" (J. W. Hightower, Ed.), p. 1125. North-Holland, Amsterdam, 1973.
33. Ostwald, W., *Chem. Betrachtungen*, Aula, No. 1 (1895).
34. Abrahamson, J., *Carbon* **11**, 337 (1973).
35. Bruce, R. H., *J. Metall. R. Coll. Sci. Technol.* **10**, 41 (1958/59).